Unusual Hydrophobic Interactions in Acidic Aqueous Solutions

Hanning Chen, Jianqing Xu, and Gregory A. Voth*

Center for Biophysical Modeling and Simulation and Department of Chemistry, University of Utah, 315 South 1400 East, Room 2020, Salt Lake City, Utah 84112-0850

Received: March 22, 2009

Hydrophobic interaction, which is believed to be a primary driving force for many fundamental chemical and biological processes such as nanostructure self-assembly, micelle formation, and protein folding, is different in acidic aqueous solutions compared to salt solutions. In this study, the aggregation/dispersion behavior of nonpolar hydrophobic molecules in aqueous solutions with varying acid (HCl) concentrations is investigated using novel molecular dynamics simulations and compared to the hydrophobic behavior in corresponding salt (NaCl) solutions. The formation of unusual weakly bound hydrophobe-hydrated proton solvation structures is observed and can be attributed to the unique "amphiphilic" characteristic of hydrated protons. This molecular-level mechanism for the acid-enhanced dissolution of hydrophobic particles also provides a novel interpretation for the apparent anomaly of the hydronium cation in the Hofmeister series.

1. Introduction

Nonpolar solutes have been known for millennia to have a notable tendency to self-aggregate in polar solvents such as water. This everyday phenomenon of phase separation, that is, the "hydrophobic effect", is believed to govern many aspects of chemical and biological function.[1] For instance, the assembly of nonpolar residues from two domains of the same protein can eventually induce the two relatively stable individual domains to fold into a collapsed globular structure by forming a prototypical hydrophobic core.[2] The undesired formation of an oil−water emulsion during oil extraction due to the presence of natural surfactants requires further steps of purification, but the water-emulsion fuel has been shown to be able to reduce the emission of hazardous oxides of nitrogen (NO_x) pollutants in addition to an improved combustion efficiency.[3] In other areas of science and technology, solvent-controlled nanoparticle self-assembly can be primarily driven by the nanoparticle hydrophobic affinity, and the efficacy of the resulting integrated device significantly relies on the precision of the assembly process.[4]

The aggregation/dispersion behavior of hydrophobic particles in water is principally determined by the interplay between enthalpy and entropy, the two components of both the solvation and the association free energy. Though the aggregation of the hydrophobic particles is typically favored entropically, it is more complicated enthalpically since both the dispersion interaction between the hydrophobic particles and with the water molecules as well as the hydrogen bonding rearrangements in the surrounding water solvent must be considered.[5] Thus, it is not surprising that the hydrophobic effect is sensitive to solvent conditions such as temperature,[6,7] existence of electrolyte cosolute,[8,9] and pH.[10−12] For example, the ambient gas solubility of butane, an aliphatic compound, can be reduced by ∼50% in 1.0 M NaCl solution when compared to that in pure water, while only a ∼10% decrease was observed in 1.0 M HCl solution.[13] In addition, urea is known to be able to induce the denaturation of a helical polypeptide chain that is otherwise relatively stable in aqueous solution.[14] Indeed, even though urea and other acidic agents, for example, trichloroacetic acid,[15] have been widely used for decades as protein denaturants, an in-depth understanding of their mechanism of structural interference remains a work in progress.[16,17] This behavior may be further complicated by the possible involvement of hydrated protons, given the low pK_a value of urea in water.

Anomaly of the Hydrated Proton in the Hofmeister Series. Vibrational sum frequency spectroscopy[18] has been used to explore the fact that the hydrophobic/water surface tension is reduced by the relative interfacial abundance of the cosolute anions. Thus, the famous Hofmeister series,[19] which qualitatively arranges cations and anions by their ability to precipitate proteins, may be rationalized by the partitioning of cations and anions between the bulk phase and the interfacial region.[18] According to this interpretation, the combination of an anion with high electronic polarizability and a cation with strong hydration affinity would be an optimal choice for dissolving hydrophobic species.

As a cation's hydration free energy is inversely dependent on its ionic radius, it is not surprising that larger cations are generally more efficient at "salting-out" (precipitating) proteins, whereas the smaller cations are generally more efficient at "salting-in" (solubilizing) proteins. However, although a hydrated excess proton (usually referred to as "hydronium") has a similar radius to the salting-out cations K^+ and NH_4^+, the solubility of hydrophobic molecules is typically enhanced by low pH conditions (see, for example, ref 14). Thus, the role played by the hydrated excess proton[20,21] in facilitating the dissolution of nonpolar solutes cannot be simply ascribed to its hydration free energy alone. A mechanism at the molecular level is needed to rationalize this apparent anomaly of the hydrated proton in the Hofmeister series and the unusual solubility of hydrophobic species in acid solution in general. The present article provides a novel explanation for this important phenomenon: one that would also seem to have broad implications. For example, the present findings may further the understanding of acid-assisted denaturation of proteins,[22] pH-induced formation of polymer micelles,[23] fabrication of highly ordered nanoparticle surfaces,[24] and the uptake of organic pollutants by acified atmospheric aerosols.[25]

* To whom correspondence should be addressed. E-mail: voth@chem.utah.edu.

10.1021/jp9025909 CCC: $40.75
Published on Web 04/30/2009

Unusual Behavior of Hydrated Excess Protons. Contrary to what is presented in much of the current literature and in most chemistry textbooks, the hydronium cation, H_3O^+, does not actually exist in aqueous solution as a "classical" cation. Instead, the hydrated excess proton exists as an ever-changing structure, with the Eigen cation, $H_9O_4^+$, and the Zundel cation, $H_5O_2^+$, as its limiting forms.[20,21,26,27] This is because the net positive charge defect created by the hydrated excess proton in water is delocalized across multiple water molecules.

In our group's previous work, an additional and unusual "amphiphilic" character for the hydrated excess proton was discovered[28] and further analyzed[29] via computer simulations, leading to the prediction that the hydrated proton would have an enhanced concentration at mixed dielectric interfaces such as the water liquid−vapor interface. This interesting behavior has received significant experimental support,[30−32] and it arises mainly because the hydrated excess proton (predominantly the hydronium structure H_3O^+) has asymmetric hydrogen bonding properties with the water solvent, strongly associating with three water molecules on one side while clashing with water hydrogen bonding on the other (lone electron pair) side. In light of this unusual behavior, one might also predict that the association of hydrated excess protons with hydrophobic solute molecules in acid solution should be quite different than the association of such solutes with more classical cations such as Na^+ in aqueous NaCl solution. In turn, these differences would lead to different solubilities of the hydrophobic species in acid versus salt solution[13] as well as different hydrophobic association behavior of the hydrophobes in these solutions. The present article provides a confirmation and an explanation of interesting prediction via computer simulation, consistent with the known experimental results. Neopentane, the smallest hydrocarbon molecule that exhibits a considerable hydrophobic aggregation effect,[10,33,34] will be the hydrophobic solute studied in the present work.

2. Methods

The multistate empirical valence bond (MS-EVB) method[20,21,35] has been employed in this work to simulate hydrated excess protons in aqueous HCl solution. The MS-EVB method simulates the explicit dynamic evolution of the chemical bond topology of the hydrated excess proton and therefore includes the positive charge defect delocalization and Grotthuss proton shuttling[36,37] through the rearranging hydrogen bond network. The MS-EVB method has been demonstrated to reliably and efficiently describe the solvation and transport behavior of the excess hydrated proton in bulk aqueous solution, the air/water interface, proteins, and proton exchange membrane fuel cells.[20,21] To facilitate the study of concentrated acid solutions with multiple hydrated excess protons, the self-consistent iterative MS-EVB (SCI-MS-EVB) method[38] has been utilized in this study. Other details of the molecular-scale model are given in the Supporting Information.

For the neopentane aqueous solution without the presence of any cosolute (denoted as Salt0), the system consisted of 8 neopentane molecules and 500 water molecules. For the three NaCl aqueous solutions with a molar ratio between NaCl and neopentane of 1:1, 2:1, and 4:1 (Salt1, Salt2, and Salt4, respectively), the systems were constructed by adding 8, 16, and 32 Na^+ cations along with 8, 16, and 32 Cl^- anions, respectively, to Salt0. For the three HCl aqueous solutions with molar ratio between HCl and neopentane of 1:1, 2:1, and 4:1 (Acid1, Acid2, and Acid4, respectively), the systems were formed by adding 8, 16, and 32 excess protons along with 8, 16, and 32 Cl^- anions, respectively, to Salt0.

The neopentane was modeled by the GAFF force field as described in the Supporting Information; an Amber-compatible force field refined by Dang[39] was used for Na^+, K^+, and Cl^-; the water molecules were represented by the simple point-charge flexible water (SPC/Fw) potential.[40] The dynamics of the excess proton were described by the MS-EVB3 model,[35] and the multiproton scenario was treated by the SCI-MS-EVB method as described earlier. For each of the four systems without an excess proton (Salt0, Salt1, Salt2, and Salt4), a 100 ps equilibration run was carried out followed by a 4.0 ns production run. For each of the three systems with an excess proton (Acid1, Acid2, and Acid4), 10 independent trajectories with uncorrelated initial configurations were obtained by equilibrating the systems for 100 ps before a 400 ps production run. For each of the seven systems, 40 000 configurations were saved during the 4.0 ns production run, given the time step of 1.0 fs and the output frequency of 100 steps. All simulations were conducted under the isothermal−isobaric (constant temperature and pressure) conditions with a target temperature of 298.15 K and a target pressure of 1 atm. Three-dimensional periodic boundary conditions were applied, and the long-range electrostatic interactions were treated by the Ewald summation with a cutoff precision of 1.0×10^{-6} (see Supporting Information for the computer code details).

3. Results

A. Hydrophobic Species in Acid and Salt Solutions. In the present study, the SCI-MS-EVB computer simulation methodology[38] coupled with the recently developed MS-EVB3 model[35] for hydrated excess protons (see Methods section) were employed to examine the solvation structure of the hydrophobic species neopentane in acidic solution. Specifically, three acidic solutions with a molar ratio between HCl and neopentane of 1:1, 2:1, and 4:1 were studied and are referred to here as Acid1, Acid2, and Acid4. For a comparison, three NaCl salt solutions with a molar ratio between NaCl and neopentane corresponding to those of the acidic solutions were also studied and denoted as Salt1, Salt2, and Salt4, respectively. For an additional comparison, a neopentane aqueous solution without any cosolute, denoted here as Salt0, was also investigated using classical molecular dynamics simulations. Moreover, to investigate the effect of the cation ionic radius and thus its charge-density dependent strength of hydration on the aggregation/dispersion behavior of neopentane, additional calculations were performed on four KCl salt solutions with a molar ratio between KCl and neopentane of 1:1, 2:1, 4:1, and 8:1. The additional calculations reveal that our qualitative conclusions below, though mainly drawn from the results of NaCl salt solutions, are not dependent on the choice of cation, although there is a difference in the threshold salt concentration that triggers a dramatic change in the solvation structure of neopentane. For the results of the KCl solution simulations, the reader is referred to the Supporting Information. It should be noted that the concentration of neopentane in all of these simulations is above the natural neopentane solubility. This is chosen to enhance the possibility of hydrophobic aggregation. The target of the present study is to compare this behavior between various concentrated salt and acid solutions, not to calculate the absolute solubilities of neopentane.

After including box-size fluctuations at constant pressure and temperature during the simulations, the mean values of electrolyte molarity were determined to be 0.81 M, 1.59 M, and

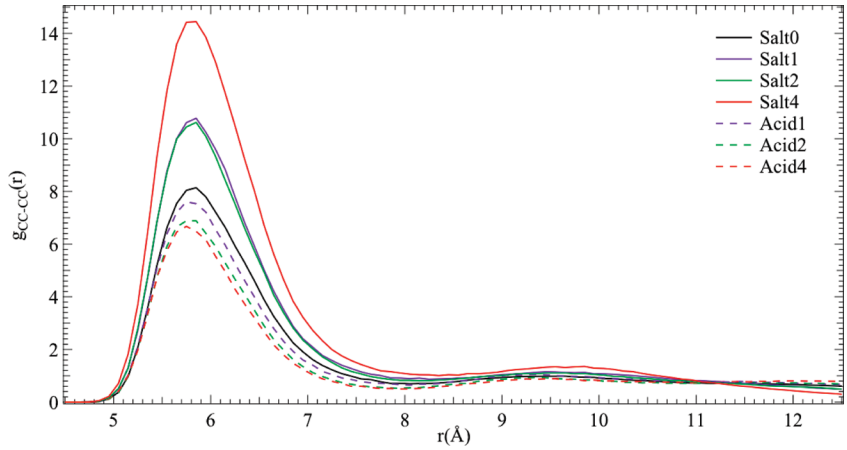

Figure 1. RDFs between CC atoms of neopentane molecules in various NaCl (Salt1−Salt4) and HCl (Acid1−Acid4) solutions. The electrolyte molarities are as follows: Salt1, 0.81 M; Salt2, 1.59 M; Salt4, 3.06 M; Acid1, 0.82 M; Acid2, 1.61 M; Acid4, 3.06 M.

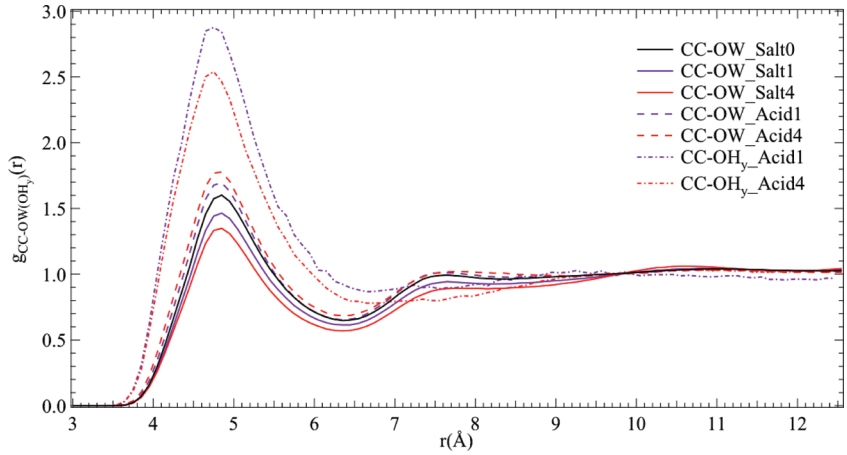

Figure 2. RDFs between neopentane CC atoms and dominant hydrated excess proton water−oxygen atoms (OH_y) and solvent OWs. The case of Salt0 is neutral neopentane solution with no salt or acid present.

3.06 M for the Salt1, Salt2, and Salt4 solutions, respectively, and 0.82 M, 1.61 M, and 3.06 M for the Acid1, Acid2, and Acid4 solutions, respectively, all with a standard deviation of 0.01 M. The nonlinear variation of electrolyte molarity upon the linear variation of the electrolyte mole fraction suggests dissimilar solvation structures in the mixture systems, which can be quantified at the molecular scale in terms of radial distribution function (RDF), $g(r)$.

The RDF between the central carbon (CC) atoms of the neopentane molecules under varying cosolute conditions is plotted in Figure 1. All of the RDFs have a common two-peak feature with the primary peak located at $r \approx 5.8$ Å that can be ascribed to the contact pair of the hydrophobic core between the neopentane molecules. The secondary peak located at $r \approx 9.4$ Å indicates the formation of solvent-separated neopentane pairs, as supported by the presence of a peak in the $g(r)$ between CC and water−oxygen atoms (OWs) located at $r \approx 7.5$ Å (Figure 2). The hydrophobic association propensity of neopentane in these solutions can be mainly assessed by the height of the primary peaks of the RDFs. In comparison to Salt0, a mild salting-out effect[41] is observed in all salt solutions except for Salt4, in which the occurrence of a strong salting-out (hydrophobic aggregation) effect[41] is indicated by the first CC−CC RDF peak to be as high as ~14.3, consistent with the results of prior simulations.[42] Remarkably, no such strong salting-out peak is observed for any of the acid solutions, not even at the equivalently high HCl concentration. In fact, in contrast to the salt solutions, the hydrophobic aggregation of neopentane was noted to decrease slightly as a function of acid concentration.

B. Solvation Structure of Neopentane in NaCl Solutions. For all of the neopentane salt solutions, Salt1, Salt2, and Salt4, the decrease of the CC−water RDF, $g_{CC-OW}(r)$, at the primary peak ($r \approx 4.8$ Å) compared to salt-free (Salt0) solution can be partially ascribed to the presence of the nearby Cl^- anion as indicated by the peaks at $r \approx 5.5$ Å in the $g_{CC-Cl^-}(r)$ RDF (Figure 3). This peak is the result of anion adsorption at the hydrophobe/water interface[43] due to the anisotropic orientation of interfacial water molecules with dangling hydrogen bonds.[44] For the case of Na^+ solvation in these solutions, which has a higher dehydration penalty when compared to Cl^-, the $g_{CC-Na^+}(r)$ RDF keeps growing before it eventually approaches the asymptotic value of unity (Figure 4), revealing an apparent partitioning of Na^+ and neopentane as expected. The slightly increased solubility of neopentane molecules in Salt2 compared to Salt1 is mainly due to the decreased dielectric constant of the solvent,[45] as a higher concentration of the dispersed salt cosolute can further stabilize the water hydrogen bond network. However, when the salt concentration reaches a higher level as in Salt4, the system separates into two phases, a "hydrophilic-rich" phase mostly consisting of NaCl and its solvated water molecules and a "hydrophilic-poor" phase mainly composed of neopentane aggregates.[42] The phase separation is indicated by a substantial drop in the primary peaks of both the $g_{CC-Cl^-}(r)$ and the $g_{CC-Na^+}(r)$ RDFs at $r \approx 5.5$ Å and $r \approx 9.3$ Å, respectively, of

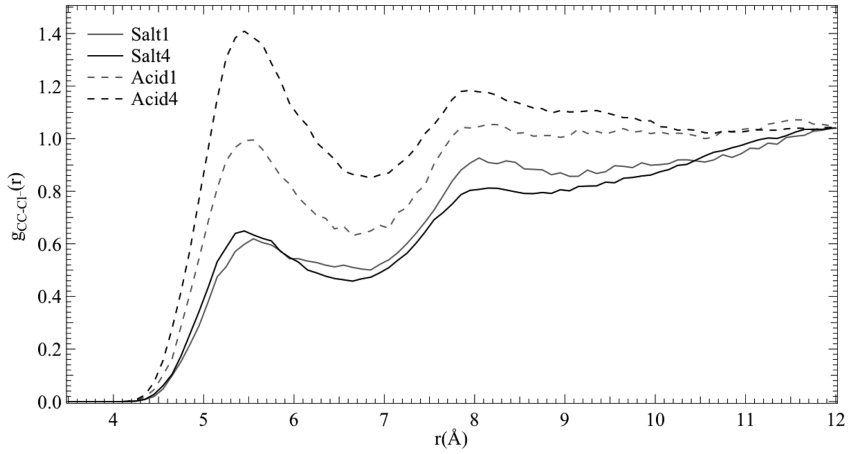

Figure 3. RDFs between neopentant CC atoms and Cl^- anions in various salt and acid solutions (see Figure 1).

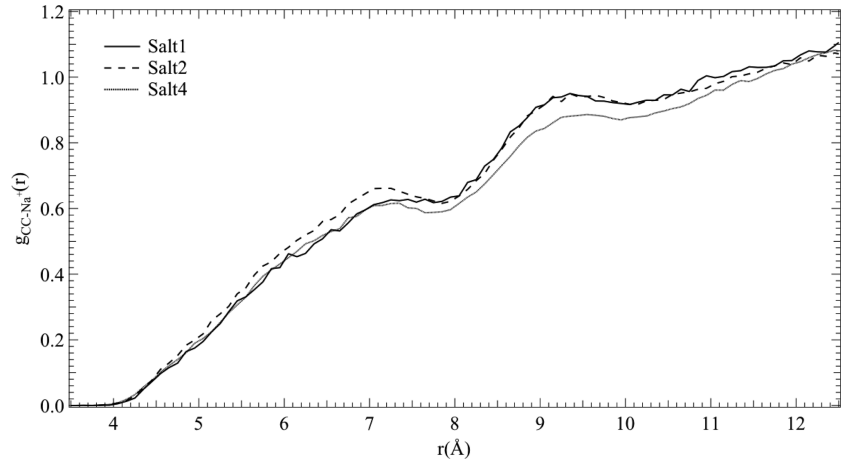

Figure 4. RDFs between neopentane CC atoms and Na^+ cations in various salt and acid solutions (see Figure 1).

Salt4 when compared to Salt1 and Salt2. This behavior is also manifested by a dewetting of neopentane, as shown by the lowering of the $g_{CC-OW}(r)$ main peak in Figure 2 for Salt4. The dewetting of neopentane is consistent with the experimental[46] and theoretical findings[47] that no less than 11 water molecules are required to form the first two solvation shells for each NaCl contact ion pair, making at least 70% of H_2O "dried out" by NaCl in Salt4. Thus, a dewetting-driven hydrophobic collapse[48] of neopentane in Salt4 becomes inevitable, as demonstrated by the singularly high first peak in the $g_{CC-CC}(r)$ RDF at $r \approx 5.8$ Å in Figure 1.

C. Solvation Structure of Neopentane in HCl Solutions. In contrast to the case of the NaCl aqueous neopentane solutions, for all three acidic solutions (Acid1, Acid2, and Acid4) the solubility of neopentane is moderately increased relative to that of the Salt0 neutral solution, as indicated by the lower values of the $g_{CC-CC}(r)$ RDF first peak at $r \approx 5.8$ Å. To investigate the "amphiphilic" effect of hydrated protons[28] on the association affinity of neopentane, the most likely hydrogen bond topology for each hydrated excess proton structure was defined in the SCI-MS-EVB simulation as the most hydronium-like structure consisting of one oxygen atom (OH_y) and three hydrogen atoms (HH). In most cases, this structure retains more excess protonic charge defect character than any other water molecule in the protonated water system. (In other publications,[20,21,28,35,38] the dominant oxygen atom of the hydrated proton structure has often been referred to as the "pivot oxygen" for technical reasons and denoted as O*; here it is denoted by "OH_y".) As manifested by the substantially higher peaks in the $g_{CC-OH_y}(r)$ RDF in Figure 2 at $r \approx 4.7$ Å and by the absence of a secondary peak, the neopentane molecules have a stronger affinity for the hydrated proton than for the water molecules, the latter being represented by $g_{CC-OW}(r)$. The marked association between the neopentane and the hydrated proton, which can be considered to be a "hydrophobe-hydrated proton core", is therefore observed in the present simulation, the possibility of which might have been hypothesized from our earlier work[28,29] concerning the "amphiphilic" enrichment of hydronium at the mixed dielectric environment of the water/air interface. It is this unusual association of the hydrated protons with the neopentane molecules that keeps the latter relatively dispersed and not aggregated (see Figure 1) and is also presumably what causes hydrophobes to have a higher solubility in acid versus salt solution as a function of acid or salt concentration. This behavior is to be contrasted with the case of the NaCl solution, particularly at the highest salt concentration.

The composition of the hydrophobe-hydrated proton core can be further quantified by the hydrated proton coordination number with neopentane within a cutoff radius of $r_{CC-OH_y} \approx 7.5$ Å, beyond which there is no ordered solvation structure. It turns out that on average there are 0.99, 1.85, and 3.29 hydrated protons in close contact with each neopentane for the Acid1, Acid2, and Acid4 concentrations, respectively, causing the hydronium-hydrated proton core to be more positively charged with decreasing pH. Further significant hydrated proton accumulation is prevented for the most concentrated Acid4 solution due to the positive charge repulsion and the more abundant accumulation of the surrounding Cl^- counterions,

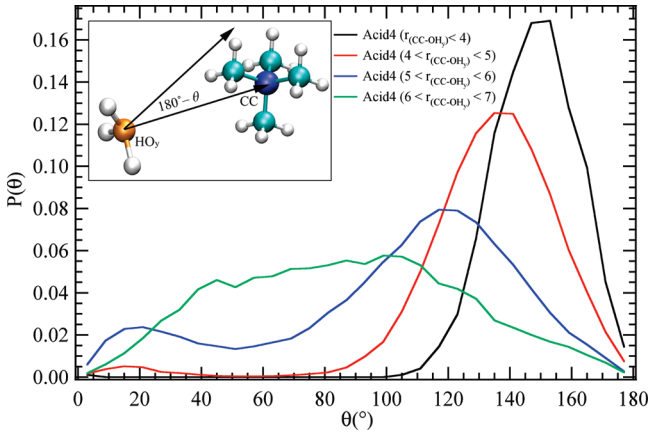

Figure 5. Probability distribution profiles of hydrated excess proton structure orientation with respect to its nearest neopentane as a function of distance (r_{CC-OH_y}) between the neopentane CC atoms and the hydrated excess proton oxygen (OH_y) atoms. See text for more details.

which in turn have a stronger net association with hydrated protons at lower pH.[49]

The interesting and unusual molecular-scale behavior of the hydrophobe in the three acid solutions compared to the corresponding salt solutions is consistent with experimental findings[13,50] which indicate that the solubility of hydrocarbon molecules is nearly invariant over a wide range of acid concentrations, whereas their solubility is quite sensitive to salt molarity in salt solutions. For the Acid1 and Acid2 solutions, the first peaks of the $g_{CC-Cl^-}(r)$ RDF are notably lower than the solvent-separated peak at $r \approx 8.1$ Å because the solvating water molecules screen the mild electrostatic attraction between the Cl^- and the moderately charged hydrophobe-hydrated proton core (the case of Acid1 is seen in Figure 2). By further increasing the HCl concentration as in the Acid4 solution, this core becomes more positively charged, eventually making the contact ion pair peak of Cl^- with the hydrated proton the dominant feature in $g_{CC-Cl^-}(r)$ (cf. Figure 3). Thus, if one considers the hydrated protons as the inner-layer surfactant for neopentane, Cl^- can be regarded as the outer-layer surfactant. This unique emulsified structure of the hydrophobe in concentrated acid aqueous solution efficiently stabilizes the hydrophobic neopentane species and inhibits its aggregation through both the electrostatic repulsion between the hydrophobe-hydrated proton cores and the hydration by the solvating water molecules of the core-bound Cl^- anions.

D. Relative Orientation of the Hydrated Protons with Respect to Neopentane. The molecular-scale structure of the hydrophobic-hydrated proton cores is interesting to examine further given the unique "amphiphilic" characteristic[28] of the hydrated proton. This structure has the hydronium lone electron pair pointing in a direction opposite to its three strong hydrophilic hydrogen bonds with the water molecules, forming the Eigen-like structure, $H_9O_4^+$. The orientation of a hydrated proton relative to a neopentane molecule can be expressed in terms of the angle θ between the vector connecting the hydrated proton structure central oxygen OH_y to the nearest neopentane CC, denoted by $\vec{R}_{OH_y-CC}$, and the vector connecting OH_y to the geometric center of the three hydrated proton structure hydrogens (CH), denoted by $\vec{R}_{OH_y-CH}$ (cf. Figure 5). The dependence of the normalized probability distribution of θ, $P(\theta)$, on r_{CC-OH_y} (Figure 5) reveals the apparent directionality of the lone electron pairs of the hydrated proton structure toward neopentane when r_{CC-OH_y} is shorter than 6.0 Å. Also, when comparing the profiles of $P(\theta)$ for Acid1, Acid2, and Acid4, the directionality of hydronium is seen to be nearly independent of acid concentration.

There are additional small peaks in $P(\theta)$ at $\theta \approx 15°$ for 4 Å $< r_{CC-OH_y} <$ 5 Å and 5 Å $< r_{CC-OH_y} <$ 6 Å that can be attributed to the electrostatic attraction between the Cl^- and the three hydrated proton hydrogens (HHs) that orients the hydrophilic direction of the hydronium toward Cl^-. For the region 6 Å $< r_{CC-OH_y} <$ 7 Å, the hydrated proton structure loses its orientational directionality toward neopentane, compared to the region 3 Å $< r_{CC-OH} <$ 4 Å, for which $P(\theta)$ is only appreciable for $\theta > 110°$ and has a relatively sharp peak at $\theta \approx 150°$. Therefore, despite the interference of these average structures by the presence of the counterion Cl^-, the hydrated proton tends to reorient its "hydrophobic" lone electron pair domain toward neopentane when they are close to each other. By adapting this orientation, the hydrophobic/water interfacial area of neopentane can be efficiently reduced, which in turn stabilizes the dispersion of neopentane. Examining the hydrated proton coordination number of neopentane as a function of the molar ratio between HCl and neopentane reveals that the hydrophobic surface of neopentane is large enough to increasingly accommodate the "amphiphilic" hydrated protons even for the (high) Acid4 HCl concentration.

4. Discussion and Conclusions

The present results taken together reveal that the enhanced solubility of hydrophobic species in acidic aqueous solutions largely originates from the existence of associated hydrophobe-hydrated proton structures. The latter are formed because the hydrated proton orients its lone electron pair toward neopentane due to the unusual "amphiphilic" character[28,29] of the former. Furthermore, the Cl^- counterions near the hydrated proton/hydrophobes attract a substantial number of solvating water molecules. This particular molecular-scale structural correlation between neopentane molecules, the hydrated protons, and the Cl^-counterions impedes the occurrence of the strong hydrophobic phase separation in concentrated acid solution. By contrast, the hydrophobic phase separation is clearly observed in concentrated salt solution. The distinctly different association/dissociation behavior of neopentane in these two solutions is visually depicted at the molecular scale in the two panels of Figure 6.

The hydrated excess proton, for which solvation and transport in the aqueous phase heavily relies on the making and breaking of hydrogen bonds with its surrounding water molecules, exhibits an unusual and directional behavior in its dominant hydrated structure. Such behavior is suggested here to have a significant impact on the hydrophobic effect and hence the association propensity between the hydrophobic solutes in acid solution. By invoking the novel molecular-level acidic emulsion mechanism described in the previous paragraph, a number of interesting phenomena can be explained or predicted. For example, anions, which are typically more polarizable than cations, are usually more crucial to the Hofmeister salting-in effect in neutral pH salt solutions because of their enhanced presence at the hydrophobic/water interface. By contrast, the amphiphilic hydronium cation (or more correctly, the hydrated excess proton) is demonstrated in the present study to be especially facile at salting-in hydrophobic solutes in acidic solutions by forming water-soluble hydrophobe-hydrated proton cores. As a result, the acid-assisted denaturation of a polypeptide composed of nonpolar residues may undergo a two-step procedure as follows: first, the association between the hydrophobic residues will be notably arrested by hydrated protons

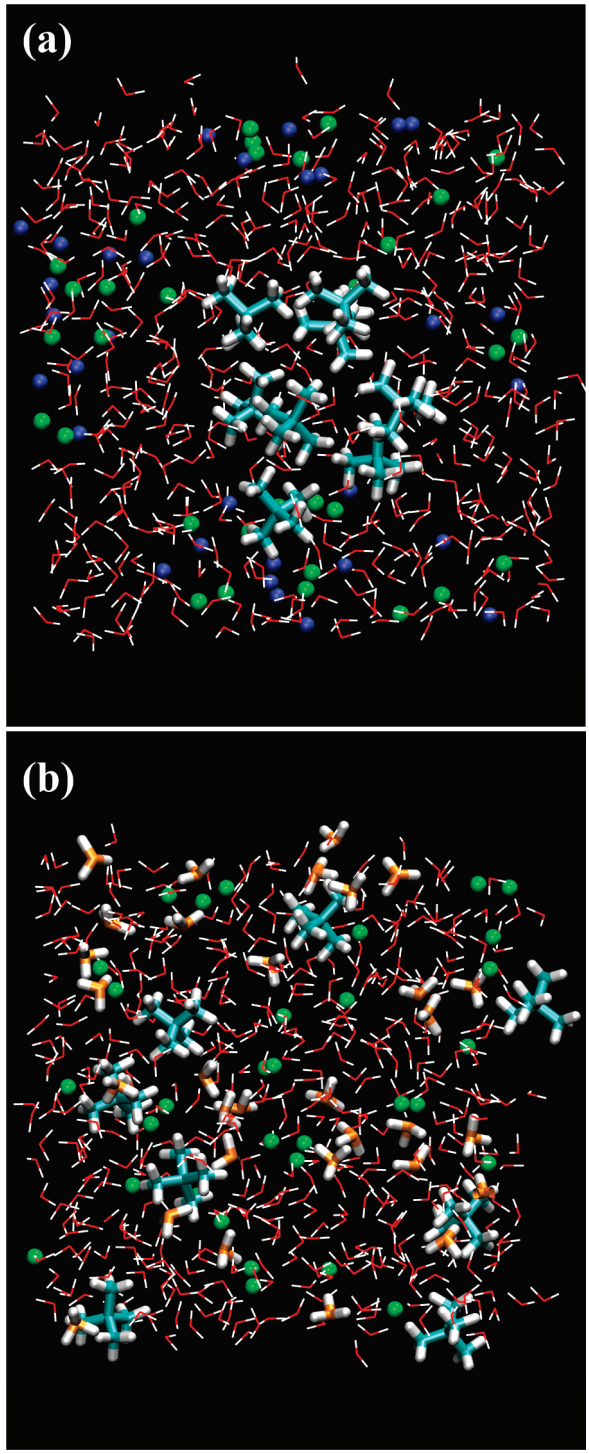

Figure 6. Representative molecular dynamics simulation snapshots of the concentrated (a) Salt4 and (b) Acid4 solutions. In panel (a), neopentane molecules are represented as licorice, while Na^+ and Cl^- are depicted as blue and green spheres, respectively. In panel (b), neopentane molecules are represented as licorice along with the hydrated excess proton structures, for which the oxygen atoms are colored orange and the Cl^- counterions are depicted as green spheres.

acting as a surfactant. Then, the polypeptide will be unfolded by electrolytic dissolution through an ion-pair like interaction. Similarly, the extent of dispersion of nanoparticles with hydrophobic domains, for which accurate control is highly desirable in the process of molecular self-assembly, may also be tunable by adjusting the pH value in solution and by varying the type of the neutralizing anions. Finally, the uptake of organic species by acidified aqueous aerosols in the atmosphere may critically depend on the molecular-scale behavior reported in this article.

Acknowledgment. This research was supported by the National Science Foundation (CHE-0719522). The computational resources for this project were provided by the National Science Foundation TeraGrid Computational Infrastructure (Grant No. TG-MCA94P017).

Supporting Information Available: Details are provided for the neopentane model parametrization, and results are presented for neopentane hydrophobic aggregation in KCl solution compared to NaCl solution. This material is available free of charge via the Internet at http://pubs.acs.org.

References and Notes

(1) Tanford, C. *Science* **1978**, *200*, 1012.
(2) Zhou, R.; Huang, X.; Margulis, C. J.; Berne, B. J. *Science* **2004**, *305*, 1605.
(3) Kadota, T.; Yamasaki, H. *Prog. Energy Combust. Sci.* **2002**, *28*, 385.
(4) Grubbs, R. B. *Nat. Mater.* **2007**, *6*, 553.
(5) Dill, K. A. *Biochemistry* **1990**, *29*, 7133.
(6) Murphy, K. P. *Biophys. Chem.* **1994**, *51*, 311.
(7) Huang, D. M.; Chandler, D. *Proc. Natl. Acad. Sci. U.S.A.* **2000**, *97*, 8324.
(8) Randall, M.; Failey, C. F. *Chem. Rev.* **1927**, *4*, 271.
(9) Ben-Naim, A.; Yaacobi, M. *J. Phys. Chem.* **1974**, *78*, 170.
(10) Wetlaufer, D. B.; Malik, S. K.; Stoller, L.; Coffin, R. L. *J. Am. Chem. Soc.* **1964**, *86*, 508.
(11) Pace, C. N.; Laurents, D. V.; Thomson, J. A. *Biochemistry* **1990**, *29*, 2564.
(12) Pace, C. N.; Laurents, D. V.; Erickson, R. E. *Biochemistry* **1992**, *31*, 2728.
(13) Hayduk, W. *Solubility Data Series: Propane, Butane and 2-Methylpropane*; IUPAC: Research Triangle Park, NC, 1986; Vol. 24.
(14) Scholtz, J. M.; Barrick, D.; York, E. J.; Stewart, J. M.; Baldwin, R. L. *Proc. Natl. Acad. Sci. U.S.A.* **1995**, *92*, 185.
(15) Kumar, T. K. S.; Subbiah, V.; Ramakrishna, T.; Pandit, M. W. *J. Biol. Chem.* **1994**, *269*, 12620.
(16) Bennion, B. J.; Daggett, V. *Proc. Natl. Acad. Sci. U.S.A.* **2003**, *100*, 5142.
(17) Hua, L.; Zhou, R.; Thirumalai, D.; Berne, B. J. *Proc. Natl. Acad. Sci. U.S.A.* **2008**, *105*, 16928.
(18) Chen, X.; Yang, T.; Kataoka, S.; Cremer, P. S. *J. Am. Chem. Soc.* **2007**, *129*, 12272.
(19) Hofmeister, F. *Arch. Exp. Pathol. Pharmakol.* **1888**, *24*, 247.
(20) Voth, G. A. *Acc. Chem. Res.* **2006**, *39*, 143.
(21) Swanson, J. M. J.; Maupin, C. M.; Chen, H.; Petersen, M. K.; Xu, J.; Wu, Y.; Voth, G. A. *J. Phys. Chem. B* **2007**, *111*, 4300.
(22) Fink, A. L.; Calciano, L. J.; Goto, Y.; Kurotsu, T.; Palleros, D. R. *Biochemistry* **1994**, *33*, 12504.
(23) Yusa, S.; Sakakibara, A.; Yamamoto, T.; Morishima, Y. *Macromolecules* **2002**, *35*, 5243.
(24) Xia, D.; Biswas, A.; Li, D.; Brueck, S. R. J. *Adv. Mater.* **2004**, *16*, 1427.
(25) Davidovits, P.; Kolb, C. E.; Williams, L. R.; Jayne, J. T.; Worsnop, D. R. *Chem. Rev.* **2006**, *106*, 1323.
(26) Tuckerman, M.; Laasonen, K.; Sprik, M. *J. Chem. Phys.* **1995**, *103*, 150.
(27) Marx, D. *ChemPhysChem* **2006**, *7*, 1848.
(28) Petersen, M. K.; Iyengar, S. S.; Day, T. J. F.; Voth, G. A. *J. Phys. Chem. B* **2004**, *108*, 14804.
(29) Iuchi, S.; Chen, H.; Paesani, F.; Voth, G. A. *J. Phys. Chem. B* **2009**, *113*, 4017.
(30) Petersen, P. B.; Saykally, R. J. *J. Phys. Chem. B* **2005**, *109*, 7976.
(31) Tarbuck, T. L.; Ota, S. T.; Richmond, G. L. *J. Am. Chem. Soc.* **2006**, *128*, 14519.
(32) Levering, L. M.; Sierra-Hernandez, M. R.; Allen, H. C. *J. Phys. Chem. C* **2007**, *111*, 8814.
(33) Huang, X.; Margulis, C. J.; Berne, B. J. *J. Phys. Chem. B* **2003**, *107*, 11742.
(34) Sobolewski, E.; Makowski, M.; Czaplewski, C.; Liwo, A.; Oldziej, S.; Scheraga, H. A. *J. Phys. Chem. B* **2007**, *111*, 10765.
(35) Wu, Y.; Chen, H.; Wang, F.; Paesani, F.; Voth, G. A. *J. Phys. Chem. B* **2008**, *112*, 467.
(36) Agmon, N. *Chem. Phys. Lett.* **1995**, *244*, 456.

(37) Cukierman, S. *Biochim. Biophys. Acta* **2006**, *1757*, 876.
(38) Wang, F.; Voth, G. A. *J. Chem. Phys.* **2005**, *122*, 144105.
(39) Dang, L. X. *J. Am. Chem. Soc.* **1995**, *117*, 6954.
(40) Wu, Y.; Tepper, H. L.; Voth, G. A. *J. Chem. Phys.* **2005**, *124*, 24503.
(41) Gross, P. M. *Chem. Rev.* **1933**, *13*, 91.
(42) Zangi, R.; Berne, B. J. *J. Phys. Chem. B* **2006**, *110*, 22736.
(43) Jarvis, N. L.; Scheiman, M. A. *J. Phys. Chem.* **1968**, *72*, 74.
(44) Du, Q.; Freysz, E.; Shen, Y. R. *Science* **1994**, *264*, 826.
(45) Chandra, A. *J. Chem. Phys.* **2000**, *113*, 903.
(46) Bouazizi, S.; Nasr, S.; Jaidane, N.; Bellissent-Funel, M.-C. *J. Phys. Chem. B* **2006**, *110*, 23515.
(47) Belch, A. C.; Berkowitz, M.; McCammon, J. A. *J. Am. Chem. Soc.* **1986**, *108*, 1755.
(48) Huang, X.; Margulis, C. J.; Berne, B. J. *Proc. Natl. Acad. Sci. U.S.A.* **2003**, *100*, 11953.
(49) Lee, S. C.; Kaplow, B. *Science* **1970**, *169*, 477.
(50) McDevit, W. F.; Long, F. A. *J. Am. Chem. Soc.* **1952**, *74*, 1773.

JP9025909